Electromagnetic Field and Transmission Characteristics of a Parallel Two-Wire Line Covered with a Three-Layer Media

Yahachi Kuboyama, *Member, IEEE,* Tsuneo Shibuya, *Member, IEEE,* and Risaburo Sato, *Life Fellow, IEEE*

***Abstract*—Electromagnetic field and transmission characteristics of a parallel two-wire line (PTWL) covered with a three-layer media were analyzed. It becomes clear that the PTWL mode will strongly couple to the natural HE_{1m} or EH_{1m} modes. At the resonance frequencies, most of the electromagnetic energy is stored in medium II region, while propagation takes place in both medium II and III. Off resonance, most of the energy is concentrated close to the PTWL. Numerical results are in good agreement with experimental results. Such a line could possibly be used as a dielectric tube antenna or, alternatively, as a band elimination filter and so on.**

***Index Terms*—electromagnetic field, mode coupling, transmission characteristics, dielectric tube waveguide.**

I. Introduction

WHEN a PTWL covered with concentric cylindrical dielectric media is excited by a balanced mode, the TEM mode of the PTWL couples strongly to the hybrid dipole mode of the surrounding dielectric media at frequencies where the HE_{1m} or EH_{1m} modes exist in the dielectric media itself. It has been confirmed experimentally that the transmission loss becomes very large and that the propagation constant for this type of line varies discontinuously at these frequencies [1], [2]. The PTWL and the Cylindrical dielectric waveguides from which it is composed have been investigated in detail respectively by various authors [3]–[6]. But there have been few analyses on the PTWL covered with multi-layered dielectric media that combine both types of lines [7], [8]. Considering the theoretical analysis of this type of the line, it is necessary to consider the axial components of the field at higher frequencies where the hybrid dipole modes in the surrounding media exist [9]–[11]. We have reported the transmission theory for these lines and obtained the propagation constants to a good approximation using the Fourier expanded current distribution on the PTWL over the angular coordinate θ [12]. However, the analysis of the electromagnetic field of these lines has not yet been carried out with sufficient rigor since they have complex boundary conditions that make it difficult to obtain the complete solution.

Manuscript received June 30, 1993; revised March 16, 1994.

Y. Kuboyama and T. Shibuya are with the Department of Electrical Engineering, Ashikaga Institute of Technology, Ashikaga, 326 Japan.

T. Shibuya is with the Department of Electrical Engineering, Faculty of Engineering, Ashikaga Institute of Technology, Ashikaga, 326 Japan.

R. Sato is with the Department of Electrical Engineering, Tohoku Gakuin University, Tagajo 985, Japan.

IEEE Log Number 9406823.

The purpose of this paper is to investigate the electromagnetic fields and transmission characteristics of these lines that have peculiar frequency characteristics. They have sharp transmission loss characteristics, similar to a resonance curve, at frequencies where the natural propagation modes of the surrounding media exist. These transmission characteristics depend not only on the shape, the size, and the permittivity of the surrounding dielectrics but, also on the shape and size of the PTWL and the relative position between the line and the surrounding media. When considering the practical applications for such a line, it becomes clear that a full field analysis is required together with a theoretical analysis of its peculiar transmission characteristics. Therefore, field plots over the cross-section of the line, the electromagnetic energy distribution in each region of the medium, the transmitted energy, and the transmission loss characteristics are analyzed using the mode-matching technique. We have analyzed a PTWL covered with a three-layer dielectric media as shown in Fig. 1. As a result, it becomes apparent that the TEM mode of the PTWL mode couples strongly to the hybrid dipole mode of the surrounding medium, at frequencies where the natural hybrid dipole modes exists in the dielectric media itself. It is also clear that a lot of energy is stored in regions II and III at these frequencies. Alternatively, the transmission power is concentrated near the PTWL, in region I, at all frequencies other than those of the natural modes. It should therefore be possible to excite the HE_{11} mode by the TEM mode of the PTWL, thus offering the possibility of using this type of line as a new type of dielectric antenna or microwave circuit. The numerical results for the radial dependence of the fields in medium II and the transmission loss characteristics are in good agreement with the experimental results.

II. Field Components

Let us consider a PTWL covered with a three-layer dielectric media as shown in Fig. 1(a). In this paper, the PTWL is modeled as an equivalent line of thin conductors with the width of $2d$ as shown in Fig. 1(b) [12]. Each region is assumed to be a lossless insulator with the free space magnetic permeability μ_0. The permittivity of the first and second layers are $\epsilon_{r1}\epsilon_0$ and $\epsilon_{r2}\epsilon_0$, respectively, and the third layer is taken as ϵ_0.

A cylindrical coordinate system using r, θ, z is chosen with the z axis lying alongside the transmission line. The z and time dependences are given by $\exp(-jhz + j\omega t)$,

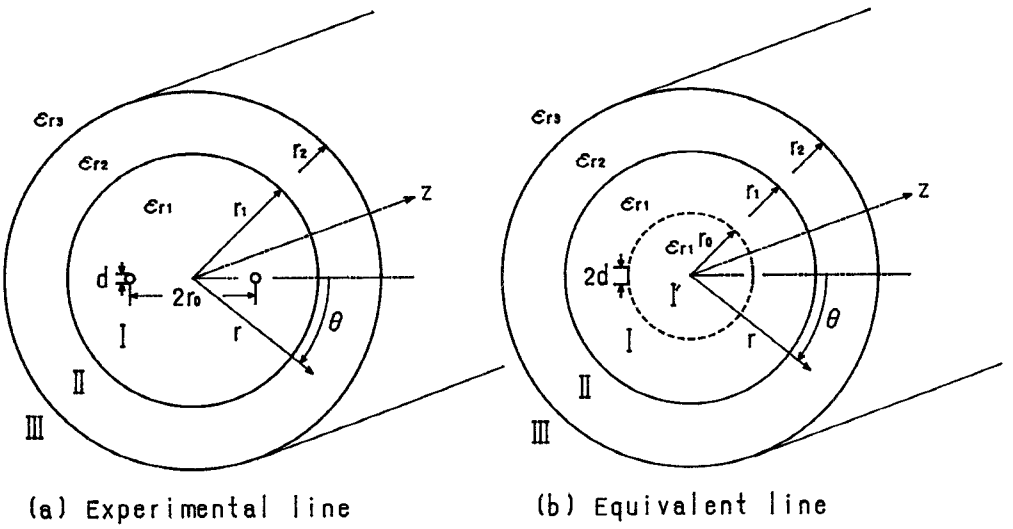

Fig. 1. Cross-section of the PTWL with a three-layer media.

where ω is the angular frequency and h is the propagation constant which is determined by the boundary conditions. The transmission mode of the PTWL is assumed to be the balanced mode. The currents $\pm I$ of the thin conductors of the equivalent line are equal and opposite to each other. Therefore, the electromagnetic fields are symmetrical about the axis of $\theta = \pm\pi/2$. The currents of each thin conductor on the radius $r = r_0$ are Fourier expanded over the angular coordinate θ. The electromagnetic fields can be expressed as a summation of the infinite series of a Bessel function. The z component of the field at each region satisfies the wave equation in cylindrical coordinates. At region I' $0 < r < r_0$,

$$E_{z0} = \sum_{n=1}^{\infty} a_{n0} J_n(\lambda_1 r) \cdot \cos n\theta \cdot F, \tag{1a}$$

$$H_{z0} = \sum_{n=1}^{\infty} c_{n0} J_n(\lambda_1 r) \cdot \sin n\theta \cdot F. \tag{1b}$$

At region I $r_0 < r < r_1$,

$$E_{z1} = \sum_{n=1}^{\infty} [a_{n1} J_n(\lambda_1 r) + b_{n1} N_n(\lambda_1 r)] \cdot \cos n\theta \cdot F, \tag{2a}$$

$$H_{z1} = \sum_{n=1}^{\infty} [c_{n1} J_n(\lambda_1 r) + d_{n1} N_n(\lambda_1 r)] \cdot \sin n\theta \cdot F. \tag{2b}$$

At region II $r_1 < r < r_2$,

$$E_{z2} = \sum_{n=1}^{\infty} [a_{n2} J_n(\lambda_2 r) + b_{n2} N_n(\lambda_2 r)] \cdot \cos n\theta \cdot F, \tag{3a}$$

$$H_{z2} = \sum_{n=1}^{\infty} [c_{n2} J_n(\lambda_2 r) + d_{n2} N_n(\lambda_2 r)] \cdot \sin n\theta \cdot F. \tag{3b}$$

At region III $r_2 < r < r$,

$$E_{z3} = \sum_{n=1}^{\infty} a_{n3} K_n(\lambda_3 r) \cdot \cos n\theta \cdot F, \tag{4a}$$

$$H_{z3} = \sum_{n=1}^{\infty} c_{n3} K_n(\lambda_3 r) \cdot \sin n\theta \cdot F. \tag{4b}$$

Where,

$$\begin{aligned} F &= \exp(-jhz + j\omega t), \\ \lambda_1^2 &= k_1^2 - h^2, \\ \lambda_2 &= k_2^2 - h^2, \\ \lambda_3^2 &= h^2 - k_3^2, \\ k_i^2 &= \omega^2 \mu \epsilon_i, \\ n &= 1, 3, 5, \cdots. \end{aligned} \tag{5}$$

J_n, N_n are Bessel functions of order n and K_n is a modified Hankel function of order n. For $h^2 - k^2 > 0$, the fields in the regions I and I' are obtained by replacing the Bessel function $J_n(\lambda_1 r)$ and $N_n(\lambda_1 r)$ by the modified Bessel function $I_n(\sqrt{h^2 - k^2} r)$ and $K_n(\sqrt{h^2 - k^2} r)$.

If the width of the strip is very small compared to the wavelength and the two conductors are sufficiently separated, the current distribution on the infinitely long strip is the same as the known electromagnetic surface charge distribution over the strip [12]. The current distribution on the strip is therefore assumed to be as follows:

$$\begin{aligned} i(\theta) &= \begin{cases} \dfrac{\pm 2 i_0}{\pi \sqrt{1 - (\theta/\theta_0)^2}} & \text{(on the strip)} \\ 0 & \text{(elsewhere)} \end{cases} \\ &= \sum_{n=1}^{\infty} i_n \cos n\theta \, (n = 1, 3, 5, \cdots), \end{aligned} \tag{6}$$

where,

$$i_n = \left(\frac{2}{\pi}\right)^2 i_0 \int_{-\theta_0}^{+\theta_0} \frac{\cos n\theta}{\sqrt{1-\left(\frac{\theta}{\theta_0}\right)^2}}\, d\theta,$$

$$\theta_0 = \frac{d}{r_0}, i_0 = -\frac{j\lambda_1 I}{(2\omega\epsilon_1 d)},$$

i_n = current expansion coefficient of order n.

The electromagnetic field is expanded in terms of twelve coefficients. Boundary conditions require continuity of all tangential components of the field, except for H_θ, which is discontinuous over the strip current. Once the latter is Fourier expanded over the angular coordinate θ, mode-matching techniques can be easily applied. If the current distribution is prescribed (as (6)), the current expansion coefficients are known and we obtain eight equations in the eight unknown field coefficients, for each mode. By setting the linear system determinant equal to zero, the modal relation is obtained as follows:

$$\begin{aligned}
&(\epsilon_{r1}v^2 - \epsilon_{r2})(w^2 + \epsilon_{r2}z^2)(v^2 - u^2)(w^2 + z^2)P_n^2 n^4 \\
&\quad - n^2[(v^2 - u^2)(\epsilon_{r1}v^2 - \epsilon_{r2}u^2) \\
&\quad \cdot (w^2 Y_n P_n - \epsilon_{r2} z^2 R_n)(w^2 Y_n P_n - z^2 R_n) \\
&\quad + (w^2 + z^2)(w2 + \epsilon_{r2} z^2)(v^2 X_n P_n + u^2 Q_n) \\
&\quad \cdot (\epsilon_{r1} v^2 Z_n P_n + \epsilon_{r2} u^2 Q_n) \\
&\quad + 8\epsilon_{r2} u^2 z^2 (w^2 + z^2)(\epsilon_{r1} v^2 - \epsilon_{r2} u^2)/\pi^2] \\
&\quad + [\epsilon_{r1} v^2 Z_n (w^2 Y_n P_n - \epsilon_{r2}^2 R_n) \\
&\quad + \epsilon_{r2} u^2 (w^2 Y_n Q_n - \epsilon_{r2} z^2 S_n)] \\
&\quad \cdot [v^2 X_n (w^2 Y_n P_n - z^2 R_n) \\
&\quad + u^2 (w^2 Y_n Q_n - z^2 S_n)] = 0
\end{aligned} \tag{7}$$

where,

$$\begin{aligned}
u &= \lambda_1 r_1, \quad v = \lambda_2 r_1, \\
w &= \lambda_2 r_2, \quad z = \lambda_3 r_2, \\
Z_n(u) &= J_n(u) + A_n N_n(u), \\
X_n &= \frac{u J_n'(u)}{J_n(u)}, \quad Y_n = \frac{z K_n'(z)}{K_n(z)}, \\
Z_n &= \frac{u Z_n'(u)}{Z_n(u)}, \\
P_n &= J_n(v) N_n(w) - J_n(w) N_n(u), \\
Q_n &= v[J_n(w) N_n'(v) - J_n'(v) N_n(w)], \\
R_n &= w[J_n'(w) N_n(v) - J_n(v) N_n'(w)], \\
S_n &= vw[J_n'(v) N_n'(w) - J_n'(w) N_n'(v)].
\end{aligned} \tag{8}$$

For $r = r_0$, and $\theta = 0$, the tangential component of the electrical field (E_z, E_θ) on the metal being equal to zero, we obtain:

$$\frac{\pi u_0}{2} \sum_{n=1}^{\infty} \left\{1 + \frac{J_n(u_0)}{A_n N_n(u_0)}\right\} J_n(u_0) N_n(u_0) i_n \cos n\theta = 0. \tag{9}$$

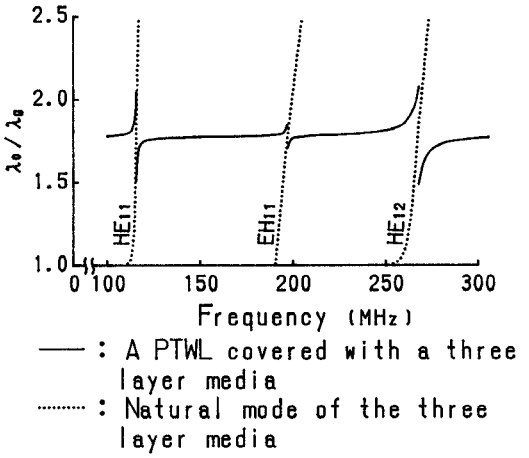

Fig. 2. Propagation constants of a PTWL covered with a three-layer media.

A_n can be obtained from (7) for each mode. We can obtain the propagation constant approximately by solving (9).

The cross-section of the line, the parameters of which have been used for the experimental and theoretical analysis, is as shown in Fig. 1. The corresponding transmission line dimensions are: $d = 0.0005, r_0 = 0.00435, r_1 = 0.0061, r_2 = 0.1125$. The mediums I, II, and III are polyethylene ($\epsilon_{r1} = 2.25$), water ($\epsilon_{r2} = 79$), and free space ($\epsilon_{r3} = 1$), respectively. It is assumed that the three-layer media are lossless. Plots of the calculated propagation constants are presented in Fig. 2, where λ_0 is the free space wavelength and λ_g is the equivalent wavelength for the transmission line.

The solid line indicates the propagation constants for a PTWL covered with the three-layer media. Near frequencies where the HE_{11}, EH_{11}, and HE_{12} modes exist in the surrounding dielectric media, the propagation constants vary discontinuously and approach those of the three-layer dielectric waveguide modes. It is considered that a radial resonance takes place between the boundaries of the media at these frequencies. Hereafter, this type of mode is referred to as a resonant mode, which is near in frequency to the HE_{1m} or EH_{1m} modes of the three-layer media. Other modes are referred to as nonresonant modes.

III. Two-Dimensional Field Plots

If the propagation constants are obtained by solving (9) and the current expansion coefficients are known, the field coefficients of (1)–(4) are determined by imposing the conditions of $r = r_0, r = r_1, r = r_2$. The relative amplitude of the electromagnetic fields for each mode are determined by the current expansion coefficient A_n. Axial and radial dependence of the fields can be easily obtained [13]. For regions near $r = r_0$, the electromagnetic field contains a large number of higher-order field components in order to satisfy the boundary condition on the conductors. For regions where r is grater than r_0, the field become nearly equal natural hybrid dipole mode, because of the higher-order fields diminish rapidly.

In order to describe the particular transmission mode of this line, two-dimensional field plots are described that compare the resonant mode and the nonresonant mode. The numerical

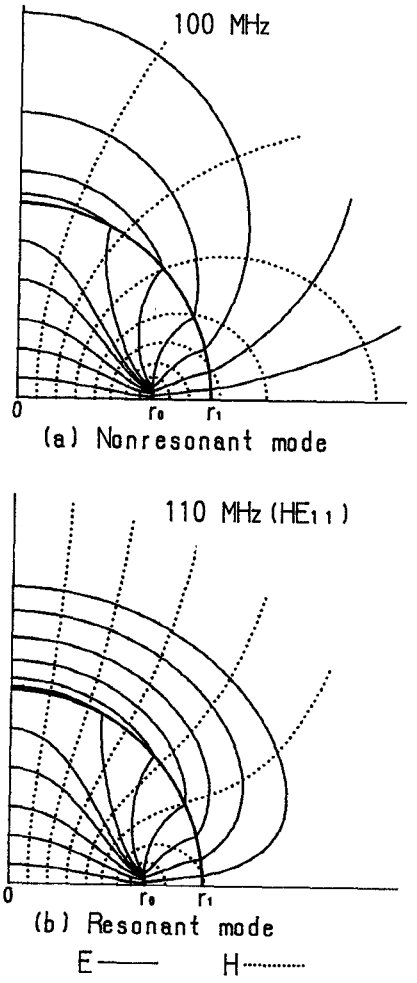

Fig. 3. Transverse field near the PTWL.

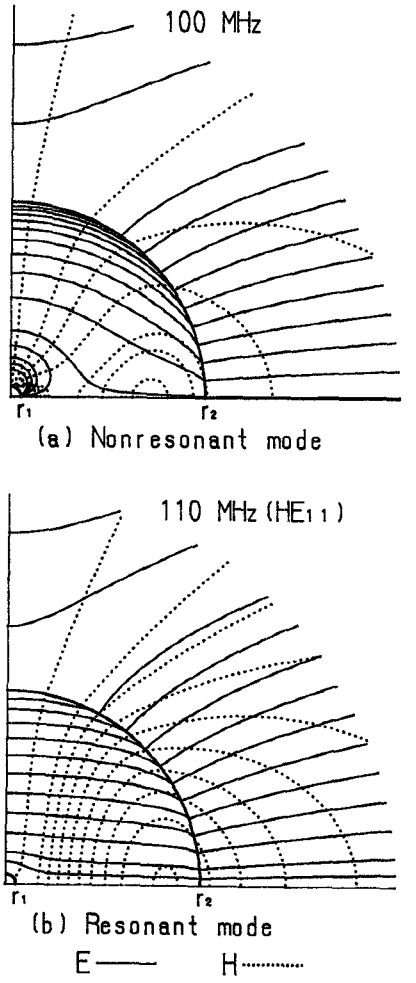

Fig. 4. Transverse field outside of radius r_1.

results are shown in Figs. 3–5. To make it easier to understand the field plots, the cross-section is divided into two areas: one is the near field of the PTWL, and the other is the field where $r > r_1$. Usually, electromagnetic field line separation is plotted in proportion to the electromagnetic field intensity. However, it is not possible to apply this method to the hybrid mode because of the fields having an axial component. Therefore, the separation of the field lines does not always indicate the fields strength. The line separation is chosen that describes the total configuration of the fields as far as it is possible. As a consequence, the field lines seem to concentrate at a certain point, but in fact do not coincide; actually they close on the different axial point.

An example of the transverse field near PTWL for the resonant mode and for the nonresonant one are shown in Fig. 3. Regardless of the resonant mode or the nonresonant one, the near field of the PTWL is nearly equal to that for the TEM mode, and, in the transverse plane, the electric field lines are nearly orthogonal to the magnetic field lines. It is observed in Fig. 3 that the electromagnetic fields concentrate to the PTWL. Orthogonality of the electromagnetic field lines in the transverse plane decreases near $r = r_1$, since the existence of the axial component for the electromagnetic field. The electromagnetic field lines of resonant mode are more different from TEM mode since the resonant modes are more influenced by the natural dipole mode.

The field plot of $r > r_1$ for which correspond to HE_{11} and EH_{11} modes are shown in Fig. 4 and Fig. 5, respectively. It shows the transition of the electromagnetic field lines from nonresonant mode to resonant mode, alternately. The electric field lines and magnetic filed lines are not always orthogonal to each other on the transverse plane; this is because of the existence of an axial field component. It is observed in Fig. 4(a) and Fig. 5(a) that the field lines for nonresonant mode concentrate near the PTWL, and spread out electromagnetic field lines into medium II and III are small. It may be said that the nonresonant modes are the forced mode by the existence of the PTWL. As shown in Fig. 4(b) and Fig. 5(b), the resonant modes are caused by the resonance between the PTWL and natural dipole modes. They are very similar to those for the natural HE_{11} and EH_{11} mode, which are shown in Appendix A for the HE_{11} mode. It can also be seen that the field lines for the resonant modes are more spread out into medium II and III than they are for the nonresonant modes.

IV. Radial Dependence of Electric Fields

Numerical and experimental results showing the radial dependence of the axial component and azimuthal component

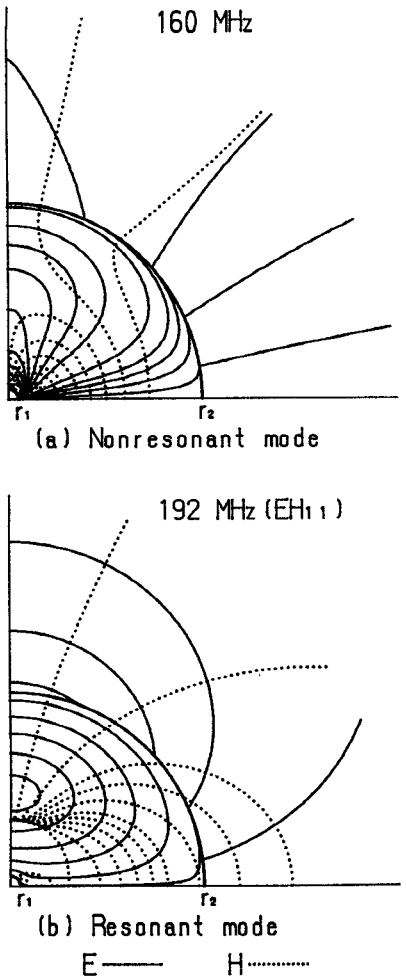

Fig. 5. Transverse field outside of radius r_1.

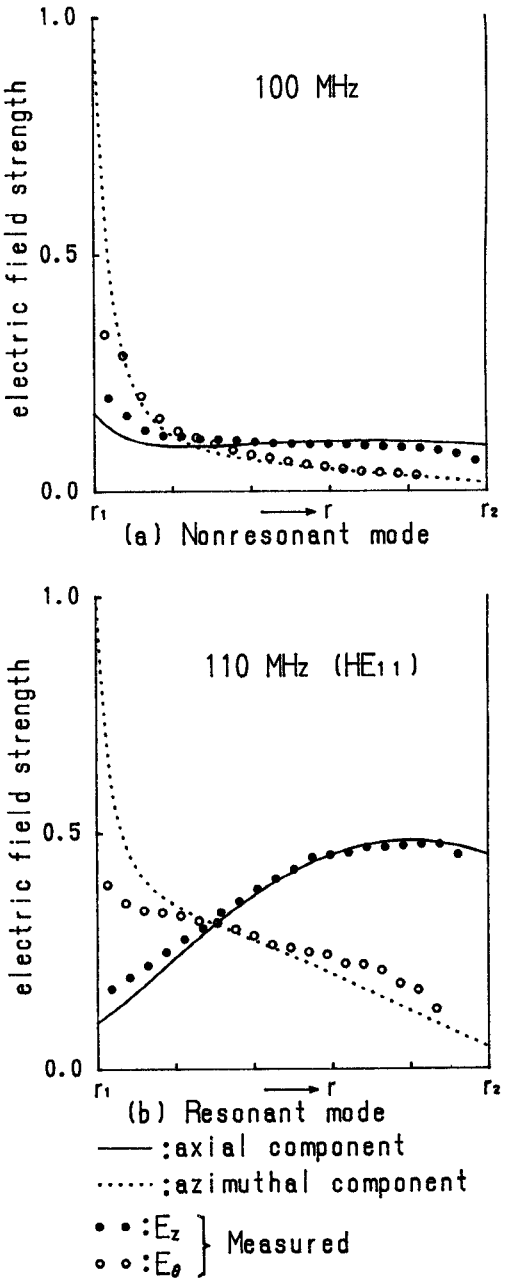

Fig. 6. Radial dependence of the fields.

of the electric fields, in medium II, are shown in Figs. 6 and 7. The azimuthal component of the electric fields, in medium II, is normalized with respect to the maximum azimuthal electric field strength. The electric field strength is measured by inserting the small dipole antenna from the surface into medium II, between the angles $\theta = 80° - 90°$. The relative magnitude of the axial component and azimuthal component of the fields vary dramatically with θ, as found from (1)–(4); for this reason, the numerical value of the axial component of the fields normalized to the measured relative magnitude of the axial component and the azimuthal component.

For nonresonant modes, the fields decrease rapidly as the radius increases. Conversely, for the resonance modes, the fields are nearly equal to the HE_{11} and EH_{11} of the natural mode of the media, and a radial standing wave is clearly observed. The level of the electric field strength for resonant modes are much greater than those for nonresonant modes. These results show that a substantial amount of the electromagnetic field spreads into medium II and that a resonance is present.

V. Transport of Energy

In order to determine the particular transmission characteristics, contour plots of the transmission power density are shown in Figs. 8 and 9. Each separation between lines represents a 4-dB difference in the transmission power density, which has been normalized to the maximum transmission power density at $\theta = 0$. The transmission power in the PTWL region is concentrated to the PTWL neighborhood regardless of whether the mode is resonant or not. However, the numerical results show that the degree to which the power is concentrated is less for resonant modes.

The transmission power density outside of medium I shows that the transmission power is diverging for resonant modes, and there are regions where the Poynting vector is negative. For nonresonant modes, the transmission power is concentrated more strongly near the PTWL. However, for resonant modes, most of the transmitted energy propagates in medium II (see Fig. 9 and Appendix B).

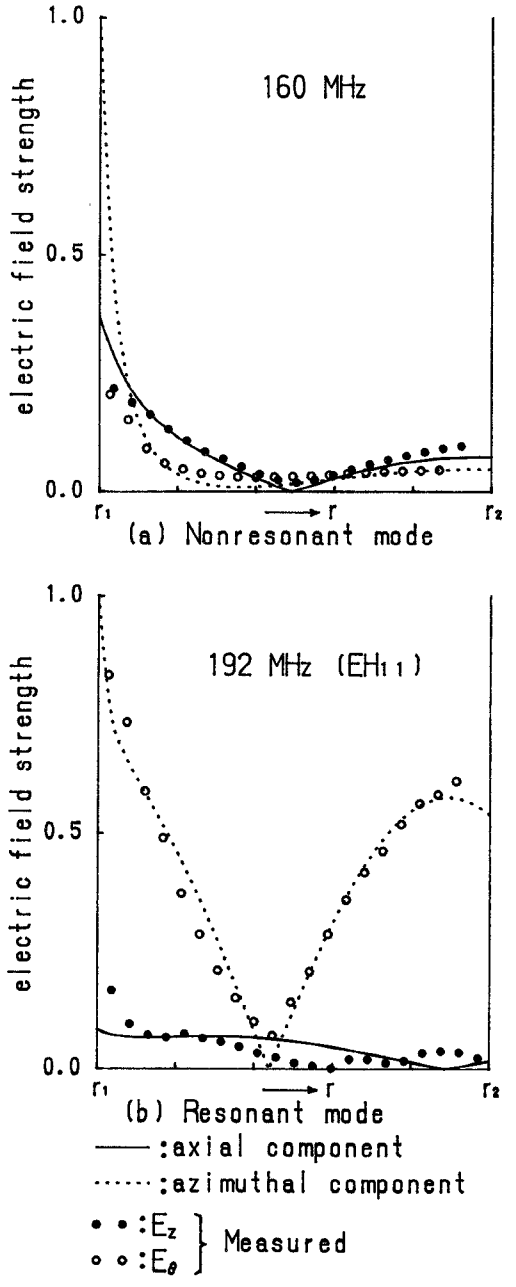

Fig. 7. Radial dependence of the fields.

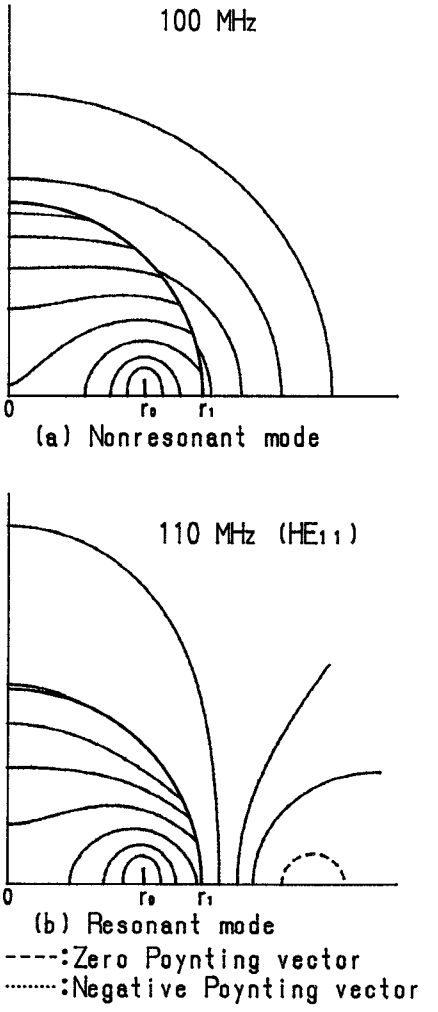

Fig. 8. Contours of the transmission power density near the PTWL.

The ratio of the transported energy in each region normalized to the total transported energy in the line is shown in Fig. 10, which shows that it varies greatly depending on whether the mode is resonant or nonresonant. For nonresonant modes, the energy propagates mainly as a TEM mode in region I. Alternatively, for resonant modes, energy transportation in region I is small; in fact, most of the energy propagates in regions II and III. A negative Poynting vector in regions II and III is observed that is mostly due to the resonant HE_{11} mode. The ratio of the transmitted energy in each region varies dramatically near the turning point of the resonance frequency.

The energy storage in each region normalized to the total transported energy in the line is shown in Fig. 11. For nonresonant modes, the electromagnetic energy is concentrated around the PTWL, and almost all the electromagnetic energy is in region I. For resonant modes, the electromagnetic field becomes nearly equal to the natural hybrid dipole mode. Therefore, a lot of energy is spread out into regions II and III. Note, that the rate of this spreading is largest for the HE_{11} mode. For higher-order modes, more energy is concentrated in medium II and less is stored in region III.

VI. Transmission Loss Characteristics

The attenuation coefficient of the dielectric-tube waveguide has been determined for TM and TE modes by Jakes [5] and, for $n = 1$ hybrid modes, by Unger [6]. This was achieved by letting the permittivity of the tube assume a complex value and by solving the characteristic equation for the complex propagation coefficient.

In this work, the well known perturbation method is used to derive expressions for the attenuation coefficient. In cases of low-loss transmission, the attenuation coefficient is given by

$$\alpha = \frac{N}{2P} = \frac{1}{2}\sum_{n=1}^{3} N_i \Big/ \sum_{n=1}^{3} P_i \qquad (10)$$

where

N_i $\omega \tan \delta_i W_i$

P_i the transport of energy in region i

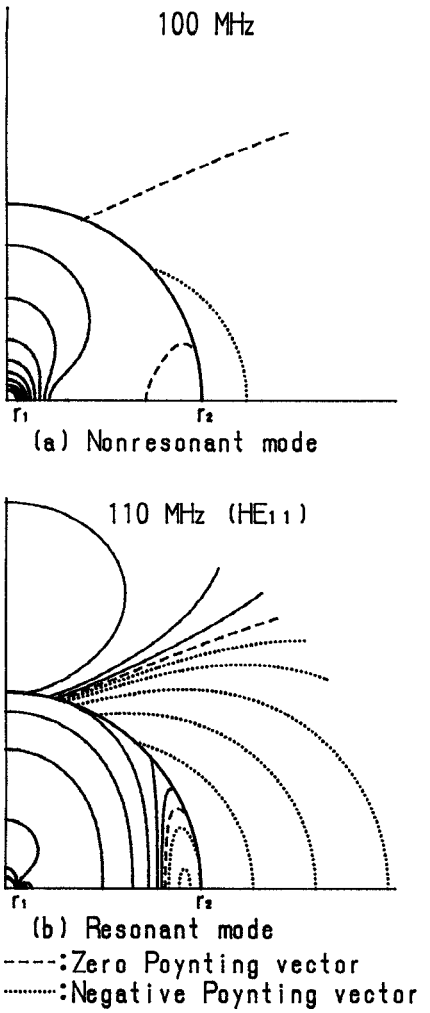

Fig. 9. Contours of the transmission power density outside of radius r_1.

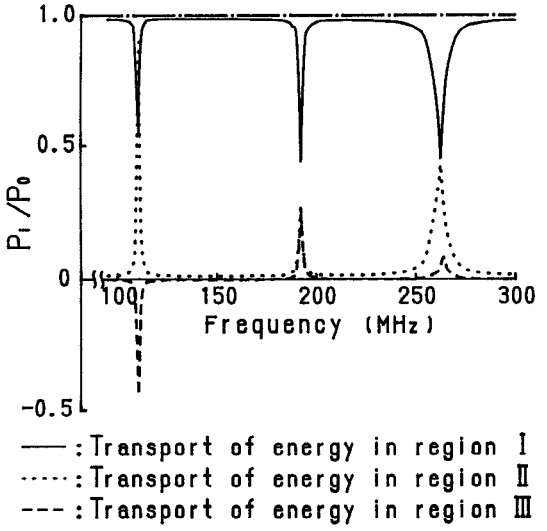

Fig. 10. Transport of energy in each region.

W_i the energy storage in region i

The line has a relatively large loss $\tan\delta_2(\simeq 0.03)$ [14] in medium II. Therefore, it is considered that the measured transmission loss for the PTWL is mainly due to this parameter.

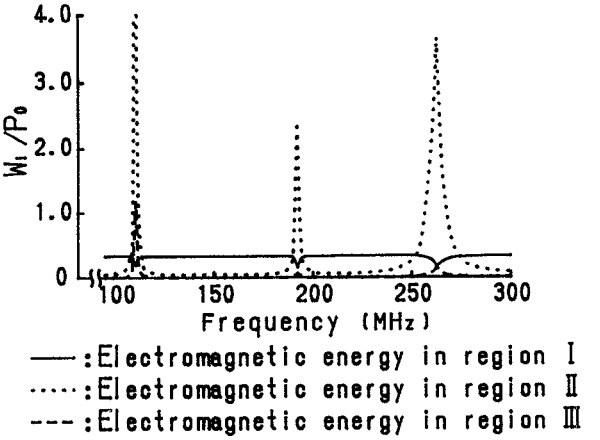

Fig. 11. Electromagnetic energy storage in each region.

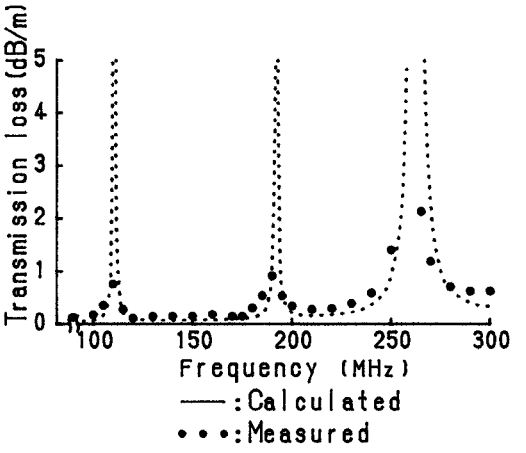

Fig. 12. Transmission loss characteristics.

The numerical result of transmission loss characteristic is in good agreement with the experimental results as shown in Fig. 12. The reason why the peak of the measured loss is not as large as the numerical value is that the resonant quality factor Q is linked to the large loss of medium II. Q is considered as being

$$Q = \frac{2\pi f(\text{average total stored energy})}{\text{average power dissipated.}} \tag{11}$$

VII. Conclusion

The numerical results for the transmission characteristics of a PTWL covered with a three-layer media are in good agreement with experimental results. At frequencies where the propagation constants of the PTWL intersect with the hybrid dipole mode of the three-layer dielectric waveguide modes, the propagation constants vary discontinuously.

For nonresonant modes, the electromagnetic energy is concentrated near the PTWL and almost all of the energy propagates in medium I. For resonant modes, the natural hybrid dipole modes are spreads out to the region II and III and most of the transported energy mainly propagates in mediums II and III.

The HE_{11} mode that has the most diverging electromagnetic field could be used as a dielectric tube antenna fed by the

balanced mode of the PTWL. Alternatively, the configuration could be used as a band elimination filter.

VIII. Appendix A

A. Field Lines for the Natural HE_{11} Mode

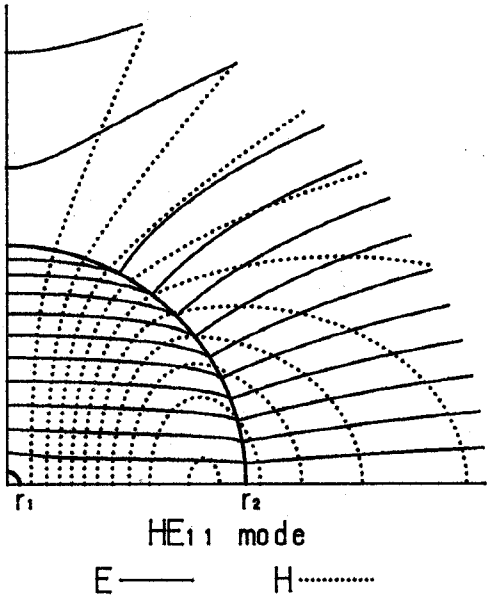

Fig. 13. Transverese fields of natural HE_{11} mode for the three-layer media.

B. Transmission Power Density Contour Plots for the Natural HE_{11} Mode that Propagates in the Three-Layer Media

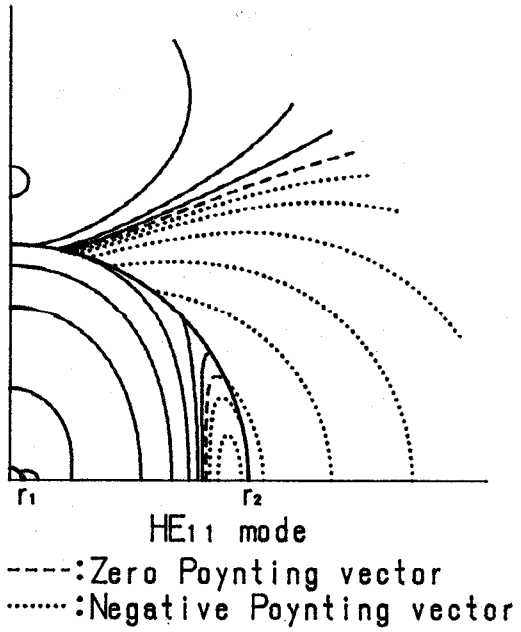

Fig. 14. Contour of the transmission power density for the natural HE_{11} mode.

Acknowledgment

The authors gratefully acknowledge helpful discussions with Prof. S. Nishida of Tohoku Gakuin Univ. and Prof. Y. Nemoto of Computer Center, Tohoku Univ.

References

[1] T. Shibuya, Y. Kuboyama, and R. Sato, "Analysis of transmission loss characteristic of Lecher wire covered with three layer media," *IECE Trans.*, vol. 53-B, no. 2, pp. 92–99, Feb. 1970.
[2] K. Toda and T. Shibuya, "Transmission characteristics (in parallel two-wire line covered with three layer media," *IECE Trans.* vol. J70-B, pp. 1092–1095, Sept. 1987.
[3] W. C. Jakes, "Attenuation and radiation characteristics of dielectric tube waveguides," Ph.D. dissertation, Northwestern Univ., IL, 1949.
[4] H. Unger, "Übertragungswerte von wellen an dielectrischen röhren," *Fernmeldetech. Z.*, vol. 8, no. 8, pp. 438–443, 1955.
[5] E. Snitzer, "Cylindrical dielectric waveguide modes," *J. Opt. Soc. Am.*, vol. 51, pp. 491–498, May 1961.
[6] M. M. Z. Kharadly and J. E. Lewis, "Properties of dielectric tube-waveguides," *Proc. IEE.*, vol. 116, pp. 214–224, Feb. 1969.
[7] Y. C. Wang, "Cylindrical and cylindrically warped strip and microstriplines," *IEEE Trans. Microwave Theory Tech.*, vol. MTT-26, pp. 23–23, Jan. 1978.
[8] C. H. Chan and R. Mittra, "Analysis of a class of cylindrical multiconductor transmission line using an iterative approach," *IEEE Trans. Microwave Theory Tech.*, vol. MTT-35, pp. 415–423, Apr. 1987.
[9] R. Sato, "Transmission theory of parallel two wire transmission line covered with multi-layer dielectric media," Tohoku Univ., Tech. Rep., vol. 30, pp. 243–259, Dec. 1965.
[10] ——, "Transmission theory of parallel-two-wire transmission line covered with multilayer dielectric media (2)," Tohoku Univ., Tech. Rep., vol. 31, pp. 41–49, June 1966.
[11] Y. Kuboyama and R. Sato, "Transmission theory of parallel two wire transmission line covered with multilayer dielectric media (3)," Tohoku Univ., Tech. Rep., vol. 33, pp.187–192, Dec. 1968.
[12] Y. Kuboyama, T. Shibuya, and R. Sato, "Transmission theory of parallel-two-wire-transmission-line covered with three layer media," *IEEE Trans. Microwave Theory Tech.*, vol. MTT-42, pp. 264–271, Feb. 1994.
[13] J. A. Stratton, *Electromagnetic Theory.* New York: McGraw-Hill, 1941.
[14] R. Von Hippel, Ed., *Dielectric Materials and Applications.* Cambridge, MA: M.I.T. Press.

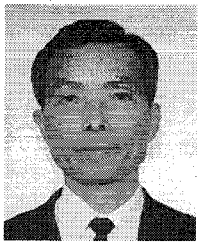

Yahachi Kuboyama (M'88) was born on February 3, 1935, in Fukuoka, Japan. He graduated Japanese Defense Academy in 1959. He received M.E. and Ph.D. degrees from Tohoku University, Sendai, Japan, in 1965, 1970, respectively.

He joined Defense Agency of Japan in 1959. From 1974 to 1977, he worked on research and development of radar system for ECCM, and from 1983 to 1987 he worked on research and development of missile system at Technical Research and Development Institute of Japanese Defense Agency. Since 1989, he has been with Ashikaga Institute of Technology, Ashikaga, Tochigi, Japan, where he is a professor in the Department of Electrical Engineering. He has been engaged in research work on transmission system covered with multi layer media and electromagnetic compatibility in digital circuits.

Dr. Kuboyama is a member of the Institute of Electronics, Information and Communication Engineers of Japan.

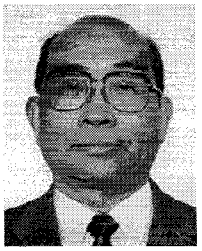

Tsuneo Shibuya (M'87) was born in Miyagi, Japan, in 1923. He received the B.E., M.E. and Ph.D. degrees from Tohoku University, Sendai, Japan, in 1952, 1963, and 1977, respectively.

He joined the Defense Agency of Japan in 1953. He had been engaged in the research and development on the radar and the airborne electronics. From 1977 to 1988, he was an associate professor at Ashikaga Institute of Technology, Ashikaga, Tochigi, Japan, and since 1988 he has been professor in the Department of Electrical Engineering at same Institute of Technology. Presently, he has been engaged in research work on transmission lines covered with multi layer media and electromagnetic compatibility.

Dr. Shibuya is a member of the Institute of Electronics, Information and Communication Engineers of Japan.

Risaburo Sato (SM'62–F'77) was born in Furukawa City, Miyagiken, Japan, on September 23, 1921. He received the B.E. and Ph.D. degrees from Tohoku University, Sendai, Japan, in 1944 and 1952, respectively.

From 1949 to 1961, he was an Associate Professor at Tohoku University, and in 1961 he became a Professor in the Department of Electrical Communication at the same university. From 1973 to 1984, he was a Professor in the Department of Information Science at Tohoku University. He is presently an Emeritus Professor of Tohoku University and Dean of the Faculty of Engineering of Tohoku Gakuin University, Tagajo, Japan. From 1969 to 1970, he was an International Research Fellow at Stanford Research Institute, Menlo Park, CA. His research activities include studies of multiconductor transmission system, distributed transmission circuits, antennas, communication systems, active transmission lines, magnetic and ferroelectric recording neural information processing, computer networks, and electromagnetic compatibility. He has published a number of technical papers and books in these fields, including Transmission Circuits.

Dr. Sato received a Best Paper Awards from the Institute of Electrical Engineers of Japan (IEE of Japan) in 1955, the Kahoku Press Cultural Awards in 1963, an award from the Invention Association of Japan in 1966, a Best paper Awards from the Institute of Electronics, Information and Communication Engineers of Japan (IEICE of Japan) in 1980, a Certificate of Appreciation of Electromagnetic Compatibility from the IEEE of USA in 1981, the Microwave Prize of the IEEE Microwave Theory and Techniques Society in 1982, the IEEE Centennial Medal 1984, the Distinguished Service Awards from the IEICE of Japan in 1984, and the Laurence G.Cumming Awards IEEE EMC-S, 1987.

Dr. Sato was the vice President of IEICE of Japan from 1974 to 1976. He has been a member of the Science Council of Japan from 1978 and a member of the Telecommunication Technology Consultative Committee at NTT from 1976. He is chairman of the Tohoku chapter of the IEEE Electromagnetic Compatibility Society and a member of the Society's Board of Directors. He is fellow of the IEEE of USA. He is also a member of the IEE of Japan, the Institute of Television Engineers of Japan, and the Information Processing Society of Japan.